SCIEPublish

Article

Enhancing the Monitoring Protocols of Intermittent Flow Rivers with UAV-Based Optical Methods to Estimate the River Flow and Evaluate Their Environmental Status

Paschalis Koutalakis *, Mairi-Danai Stamataki and Ourania Tzoraki

Department of Marine Sciences, University of the Aegean, 81100 Mytilene, Greece; marm16023@marine.aegean.gr (M.-D.S.); rania.tzoraki@aegean.gr (O.T.)

* Corresponding author. E-mail: p.koutalakis@aegean.gr (P.K.)

Received: 18 September 2023; Accepted: 23 November 2023; Available online: 27 November 2023

ABSTRACT: Temporary streams are a key component of the hydrological cycle in arid and semi-arid regions, but their flow is highly variable and difficult to measure. In this paper, we present a novel approach that could be used to assess the flow of temporary streams this allowing to characterize their environmental status. Specifically, we apply the Image Velocimetry (IV) method to estimate surface velocity in temporary streams using Unmanned Aerial Vehicles (UAVs) equipped with optical sensors (IV-UAV method). The IV-UAV method enables the easy, safe and quick estimation of the velocity on the water's surface. This method was applied in different temporary streams in Lesvos Island, Greece. The results obtained indicate that the IV-UAV can be implemented at low discharges, temporary streams and small streams. Specifically, the water depth ranged from 0.02 m to 0.28 m, while the channel width ranged from 0.6 m to 4.0 m. The estimated surface velocity ranged from 0.0 to 5.5 m/s; thus, the maximum water discharge was 0.60 m^3/s for the largest monitored stream of the island. However, there were many occasions that measurements were unable due to various reasons such as dense vegetation or archaeological sites. Despite of this, the proposed methodology could be incorporated in optical protocols which are used to assess the environmental status of temporary streams of Mediterranean conditions. Finally, this would become a valuable tool for understanding the dynamics of these ecosystems and monitoring changes over time.

Keywords: Environmental flow; Intermittent flow; Mediterranean conditions; Optical protocol; Surface velocity; Temporary streams; Unmanned aerial vehicles

1. Introduction

Accurate river discharge data play a critical role in hydrological processes and they are necessary for a variety of practical hydrological applications, such as hydrological modeling for water resources assessment and management, reservoir operation and flood management, design of hydraulic infrastructures, environmental changes and riparian areas adaptation, strategic planning and policies for civil protection and water management activities [1–4]. Such data is essential in arid or semi-arid regions, especially in islands, where flash flood warning systems are still limited and not effective due to the limitation of discharge monitoring and observational networks [5].

Intermittent and ephemeral streams (IRES) are dominant in arid or semi-arid regions [6]. The flow in ephemeral streams is episodic while intermittent streams are characterized by flow cessation, usually followed by a complete drying of the channels [7,8]. These temporary streams constitute more than 50% of the global hydrologic network while this percentage is growing due to the impacts of the climatic crisis which alters the status of the majority of rivers from perennial to intermittent [9]. IRES are prevalent in many countries across Europe but also in Mediterranean countries outside Europe; reaching a 26% coverage for the south Mediterranean terrestrial area [10,11]. IRES are also found in the headwaters of many drainage basins in wetter climates [12]. The area of the watersheds of IRES that drain into the sea is estimated to be around 43% of the total area of Greece excluding the mountainous tributaries (steep slopes) on the karstic geology [13,14]. The lack of IRES' monitoring is particularly acute on islands [15]. Furthermore, the water bodies of the Greek islands reveal high variability of the streamflow and water supply through the year and this would be intensified due to climate change [16–18].

The flow regimes (e.g., frequency, magnitude, duration, and timing of flow events) of IRES are very vulnerable [19]. Climate is the main force affecting flow regime of IRES through precipitation, temperature and wind [20]. In addition, slope, geology, and

https://doi.org/10.35534/dav.2023.10006

geomorphology are factors that influence the physical and biological attributes of IRES [21]. Furthermore, humans alter the flow regimes of IRES by altering runoff patterns in catchments through various land uses and by direct impacts on instream flows from dams and extraction of surface and ground water [22]. Anthropogenic threats to IRES can be broadly classified into hydrological, physical, chemical, and biological alterations on the flow regime [23]. Anthropogenic litter, especially macro and micro plastic pollution, is also a serious threat of IRES ecological and environmental status [24]; thus monitoring, evaluation and hierarchy of their environmental status is a "must".

The environmental status assessment requires a lot of complex physical data collection, measurement of variables based on the datasets, and analysis of the produced variables [25]. This is difficult to be assessed without a protocol providing guidelines to be followed [26,27]. Such protocols for environmental measurements exist focused on different aspects e.g., terrestrial invertebrate functional traits [28], carbon stock in forests [29], for GIS applications [30], for UAV missions and pre-flight conditions [31,32]. There are also protocols focused on specific areas; e.g., for monitoring protecting areas by UAV technology [33], for marine debris assessment [34], for lakes and other standing waters [35] for coastal areas which incorporate the morphology of the study area, the environ-mental conditions, and flight parameters [36,37], for dams constructed on stream network and how affect environmental flows [38], among others.

Unmanned aerial vehicles (UAVs or commonly drones) have been widely used for both terrestrial applications but also over water resources [39]. There are many suitable UAVs with either lightweight cameras or custom and heavily equipped ones. Different instruments and sensors can capture RGB (red-green-blue) color standard pattern, multispectral, or hyperspectral images and even LIDAR (LIght Detection and Ranging) datasets [40]. These tools can provide remote sensing capabilities and of high-resolution photogrammetric products to map and monitor riverine environments and to further analyze different environmental characteristics using innovative technologies (e.g., machine learning) [41]. UAVs used on water resources studies are mainly focused on coastlines, perennial rivers, lakes and/or reservoirs with limited applications on sea or IRES [42–45].

Recent developments on photogrammetry and image-based velocimetry monitoring techniques (IVMT) offer a great potential for IRES monitoring [46,47]. These techniques offer massive, easy, safe and low-cost measurements in real time, at any flow conditions and at high spatial resolution [48]. There is a significant development of optical-based monitoring methods during the last years [49,50]. IVMT use a sequence of images that can be captured by various ways such as digital permanent gauge cameras installed close to the river, mobile devices with operators standing on the banks and on bridges, or cameras attached to UAVs [51–56]. The surface velocity field in IVMT is indirectly obtained by measuring the velocity of floating tracer particles, naturally present (e.g., foam, light de-bris, vegetation, wood, surface waves) or artificially introduced to the flow [57]. The water surface is recorded by cameras, through a sequence of consecutive frames (extracted from a video), reconstructing the local flow velocity starting from the identification of the tracer particles displacements between pairs of subsequent frames. Among the various IVMT applications [58–60], there are three different approaches that have gained wide consensus for natural rivers monitoring: (a) the large-scale particle image velocimetry (LSPIV); (b) the particle tracking velocimetry (LSPTV) and (c) the Space-Time Image Velocimetry (STIV) technique [61]. These techniques were originally developed for laboratory scale experiments under controlled conditions e.g., as particle image velocimetry (PIV) and particle tracking velocimetry (PTV) techniques [62]. LSPIV is characterized by the Eulerian point of view, while LSPTV uses a Lagrangian point of view [63]. The two techniques have several common characteristics, while the main difference is that LSPIV estimates the velocity at image sub-regions, while LSPTV reconstructs the trajectory of individual particles transiting in the field of view [64]. Furthermore, STIV identifies the brightness variation in a searching line set parallel to the main flow direction compared to the continuous images [65]. This method is more suitable, when the stream flow is not complex, while it can provide a high calculation speed and computation efficiency [66]. All above methods need floating tracers in order to be implemented [67]. In the field applications, tracer particles must be ecologically inert as in most situations it is not possible to be recovered and re-used (e.g., tree leaves) [68]. In addition, they need to be large enough to be visible and captured by the UAV's camera. Generally, the necessary steps of IVMT implementation require the following [69]: (a) seeding of tracers with adequate geometry and density; (b) recording of images with an adequate temporal resolution; (c) processing (i.e., elaboration of recorded images including pre-processing procedures such as images stabilization, orthorectification, image enhancement if needed, and estimation of the tracer displacements between pairs of consecutive images; and (d) evaluation of velocity data with post-processing.

The estimation of the discharge is also possible by combining the bathymetry of a river cross section with the calculated surface velocity field [70]. Image-based methods can be applied in both gauging and ungauged sites. At a gauging station, discharge measurement can be easily estimated by using a water depth meter while at an ungauged site, flow discharge can be obtained by more in-situ cross-channel measurements [71,72]. Furthermore, image-based methods can be applied to existing surveillance video images taken in cities to monitor surface flow-based urban flooding [73]. There are various studies that combined a UAV with image-based methods (IV-UAV) to successfully estimate the surface velocity or discharge of a river based on low-altitude aerial imagery [74–77]. When utilizing IV-UAV, the images can be captured parallel to the water surface but in most cases the camera is at an oblique angle in regard to the measurement surface or with a wide-angle lens [78]. This technique induces the error of perspective distortion which is the direct result of camera placement in relation to an object [5]. For this reason, the captured images need to be ortho-rectified before image interrogation by using a few selected ground control points (GCPs), that can be either natural (trees, rocks, etc.) or man-made objects (buildings, pillars, targets, etc.) that are included in the images [79]. Sometimes IV-UAV

is the only available method in places where accessibility is limited, harsh or even dangerous [80]. Another advantage of IV-UAV implementation is that if images are captured perpendicular to the stream, the image orthorectification is not required [81].

The scope of this study was to implement IV-UAV technique at different locations of IRES in the Greek island of Lesvos. These techniques are frequently tested in rivers and streams that have perennial flow all the year and as a consequence there are limited studies focused on headwaters and temporary streams, based on our knowledge and a short review we have performed [82–87]. The datasets collected to monitor the water resources of Lesvos Island for both quality and quantity. These results will be further investigated and utilized in order to develop a UAV-based environmental protocol focused on IRES that will incorporate the water state, velocity and discharge along other parameters.

2. Materials and Methods

2.1. The Study Area

Lesvos (Lesbos) Island is the third largest Greek island, located on North East Aegean Sea, occupying an area of 1632 km^2 (Figure 1) [88]. Lesvos consists of a separate regional unit of the Northern Aegean region and its capital is Mytilene (Mytilini), located on the east of the island. The island's human population is 85,330 according to 2011 census [89] while last years has received a huge wave of refugees and migrants [90,91]. It is also a popular touristic destination with many unique sites to be visited. As an example, the Lesvos Petrified Forest Geopark is a worldwide acknowledged area located on the western peninsula of Lesvos Island that due to the exposed fossilized tree trunks, it was declared a National Natural Monument in 1985 [92]. The climate of Lesvos is dry in summer, and mild in winter [93]. The median annual temperature is 17.6 °C; the average humidity is around 65%; winds are generally mild (<3 Beaufort) with a northerly prevailing direction (25.25%) and regular sea breezes (meltemia, 10%); the rainfall has a range between 400–500 mm per year but it is limited in duration [94]. Lesvos receives around 1 billion m^3 of freshwater annually, out of which only 13% infiltrates and recharges the underground aquifers; 62% corresponds to the evapotranspiration and the remaining 25% ends up as surface runoff [95]. The stream network of the island belongs to an IRES network, characterized by a seasonal flow that only exists for a period of 5–6 months (from November to April) as the majority of Mediterranean streams. 143 million m^3 of water undergoes infiltration and this amount varies with the local scale precipitation features (intensity, duration, frequency of appearance) as well as the physiographic and geologic features of the area (extent, slope, ground cover, soil permeability, underground layers capacity) [96].

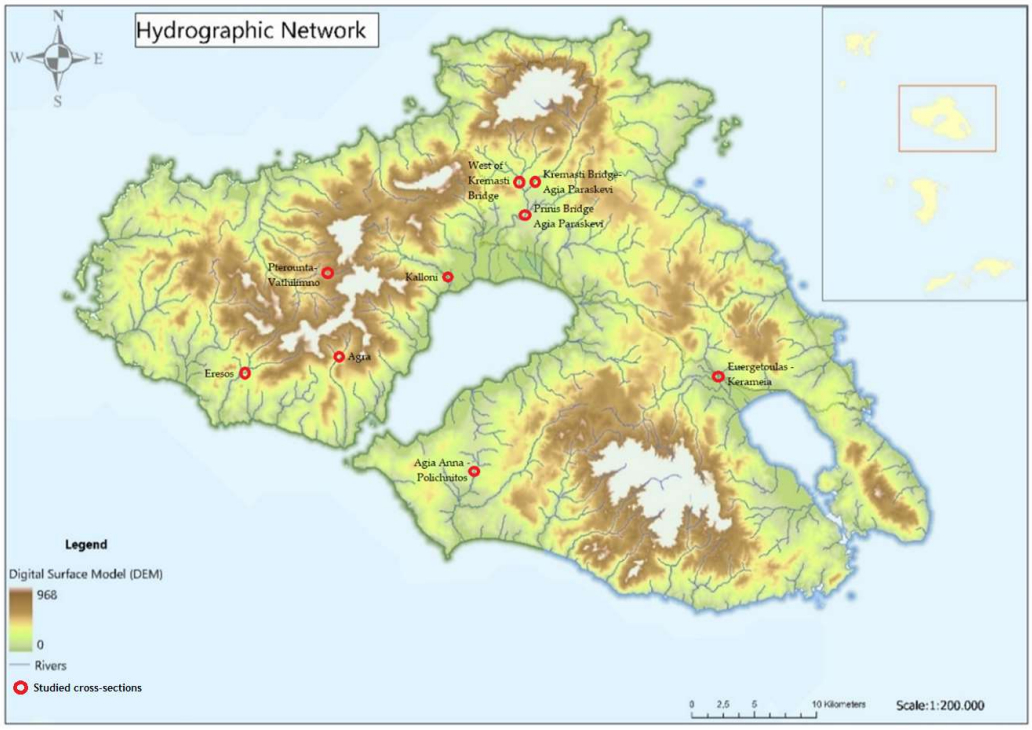

Figure 1. The digital elevation model, the hydrographic network of Lesvos Island and the locations of the studied cross-sections (red circles).

The following figures are representative of the stream network found in Lesvos Island (Figure 2). Fieldwork was conducted on different cross sections of various streams located in Lesvos Island (Table A1). Natural tracers were selected (e.g., tree leaves/brunches or natural flow patterns) to detect the motion of surface water. Surface flow velocities were collected via the DJI Mavic 2 Pro (vertical video) while cross section measurements were done by using a laser distance meter and a tape measure. Free

software (PIVlab) has been employed for preliminary treatment (orthorectification and format conversion) of video-recorded images as well as for LSPIV application.

Figure 2. Representative UAV-captured images of the stream network in Lesvos (**a**) Vatera beach, (**b**) Evergetoulas—Kerameia, (**c**) Pterount—Vathilimno, (**d**) Eresos (**e**) Kremasti Bridge—Agia Paraskevi and (**f**) Prinis Bridge—Agia Paraskevi.

2.2. The Field Survey

In this study a quadcopter, the DJI Mavic 2 Pro (DJI, Shenzhen, China) was used to acquire video of surface velocity at different sections of IRES network in the island of Lesvos. The specific UAV is a powerful quadcopter capable to fly over large areas as its battery life is 30 minutes. The DJI Mavic 2 Pro UAV equipped with Hasselblad 20 megapixels digital camera and a complementary metal-oxide-semiconductor (CMOS) sensor was utilized to capture a stable video over the water surface. The specifications of the UAV are depicted in Table 1 [97]. The UAV is connected via Wi-Fi to a smartphone/tablet and can be operated through the official application DJI GO 4. The "Tripod Mode" is an intelligent flying mode option that reduces the speed of the UAV, and the video is stable and smooth; appropriate for image-based methods analysis. The UAV hovered at different heights above the water paths and captured video at orthogonal view (flat surface water surface) of about 60 seconds. Cross sections measurements of the river width for calibration scopes were achieved by using a typical tape measure. The ground control points (GCP) included natural points (e.g., trees, rocks), human constructions (e.g., fence, waste water treatment plant) and artificial marks (e.g., black/white targets in A4 size) and all were used in order to orthorectify and calibrate the produced results. The necessary GCPs were measured mostly along the side of each stream by using at least 4 points for stabilization. If possible, by the absence of vegetation cover or other obstacles, we measured also the corners of the captured frame in each flight. Surface velocity was measured by an expert software. Unfortunately, it was impossible to verify with measurements using e.g., a current meter or another method; as in most cases the water depth was so low for the functionality of the propeller. The surface velocity was verified by the

floating method; a traditional surface velocimetry method by measuring the time + distance covering the throwing particles in a subjective manner (human eye observation and chronometer). The results from the floating method were identical to those produced by the IV-UAV method. Finally, for the estimation of the maximum water discharge, we considered the wide rectangular nature of the cross-sections that were measured by field survey using a tape measure.

Table 1. The DJI Mavic 2 Pro specifications *.

UAV Specifications	Camera Specifications
Takeoff weight: 907 g	Sensor: 1″ CMOS
Dimensions (length × width × height): 322 × 242 × 84 mm	Effective pixels: 20 million
Max flight time: 29–31’	Shooting range: 1 m to ∞
Battery capacity: 3850 mAh Battery Voltage: 15.4 V	ISO range Photo: 100–3200 (auto)
Max speed (sport): 72 km/h	Image size: 5472 × 3648
Satellite positioning: GPS/GLONASS	Format: JPEG/PEG/DNG (RAW)
Hover accuracy range: Vertical ± 0.1 m Horizontal ± 0.3 m	Gimbal Stabilization: 3-axis (tilt, roll, pan)
Max transmission: 6000 m	Lens FOV: about 77° 35 mm Format Equivalent: 28 mm

* from https://www.dji.com（accessed on 1 April 2023）

2.3. The Preprocessing of Video/Images

Firstly, the captured video was pre-processed for the reduction of various undesired errors such as lens distortion and shaking of the camera (shift, rotation and focus). PTLens and Hugin software were utilized to remove lens distortion while tilt (if appeared) was removed by using the “Deshaker Toolbox”. PTLens, although it is a commercial software, it is one of the most-used programs [98]. The tool has a Windows graphical user interface (GUI) but also works as a shareware add-on for Panorama Tools that automatically corrects for vignetting, pincushion distortion and barrel distortion [99]. Hugin is a graphical user interface (GUI) for Panorama tools providing a wide range of advanced features including the lens distortion correction [100]. Hugin also supports the use of masks to exclude unnecessary parts of images, or on the contrary to include the desired parts of images [101]. The Deshaker toolbox is a widely recognized image stabilizer plugin produced for the popular video player VirtualDub [70]. The tool uses a high-performance image-based approach to stabilization based on a multi-resolution search (matching algorithm) by firstly determining the optimum parameters and secondly stabilizing the video [102]. The consecutive frames of the video were exported in images of 8bits (black and white color) via the KMPlayer software. To perform the analysis, a part of all frames was selected (few seconds). The frame rate was 33.33 based on the video fps.

2.4. The Image-Based Velocimetry Analysis

PIVlab was selected for the needs of the current research among various software developed for image-based velocimetry applications as reported by a software review [44]. PIVlab was selected because it is an open-source toolbox based on Matlab environment, developed by Thielicke and Stamhuis (2014) [103]. The PIVlab was developed to analyze the flapping flight of birds [104] but it was further utilized with great efficiency in many research fields including river velocimetry [47,105–109]. PIVlab input data are sequences of images between two available modes: mode 1 (i.e., 1-2, 2-3, 3-4, etc.), so that the second image of each analyzed pair of images is also the first of the successive one; mode 2 (i.e., 1-2, 3-4, 5-6, etc.), so that the cross-correlation analysis is applied only once per each image [110]. The PIVlab consists of three main steps: (a) pre-processing; (b) image evaluation; (c) post-processing [111]. There are various pre-processing techniques to enhance images quality and increase the tracers’ recognition such as histogram equalization, intensity high-pass and intensity capping. The software provides the possibility to choose between two different correlation algorithms to evaluate the images: (a) DCC (Direct Cross-Correlation) and (b) FFT-CC (Fast Fourier Transform Cross-Correlation). Both are based on a cross correlation of small sub-images (interrogation areas, IAs) of an image pair [112]. The first one computes the correlation matrix between corresponding IAs in the spatial domain while in the second option, the correlation matrix is computed in the frequency domain using FFT [113]. The DCC option produces more accurate results, especially when flow motion is not unidirectional, but FFT is faster [114]. The accuracy of the FFT approach can be increased by running several passes on the same dataset [115]. The post-processing phase includes three steps: (a) filtering velocities and removing possible outliers; (b) replacing missing vectors through a data interpolation technique based on a boundary value solver for interpolation; and, finally, (c) removing measurements noise by applying a data smoothing technique based on a penalized least squared method [116,117]. Pre-processing was performed by using CLAHE algorithm of 20 pixels for the window size while PIV setting was based on the FFT-CC option. Multi-pass window deformation was applied with two interrogation passes: (i) 64 to 32 pixels^2 and (ii) 32 to 16 pixels^2. Both unreliable high vectors and misleading riparian vectors were deleted during the post-processing of the images. A calibration of images was applied as the pixels are converted to real distances of known physical distances among the control points.

3. Results

In this section, we focus on examples of IV-UAV implementation that were obtained with the RGB camera of the UAV platform on different IRES cross-sections in the Lesvos Island (see Figure 1 and Appendix). The cross-sections represent various environments based on the streambed material, vegetation and slope (Figures 3–11). In all of them the presence of water was visible and adequate to perform the IV-UAV methodology. Only at the Prinis Bridge—Agia Paraskevi cross section, the visibility of water column was poor due to the higher depth (0.60 m) and the flowing water. In other cross sections (Kalloni, Agra, Pterounta-Vathilimno, Eresos, West of Kremasti Bridge) the water depth was very low due to the period the measurements done. In all case studies the water visibility was very good and in cases (e.g., Agia Anna-Polichnitos, Kaloni, and Kremasti Bridge-Agia Paraskevi) fauna was also recorded such as frogs, turtles, snakes and insects. In cross-sections where the ground material was concrete, the water visibility was in good conditions and there was no vegetation at all. The Table 2 includes the cross-section measurements, the estimated surface water velocity by implementing IV-UAV methodology and the water discharge.

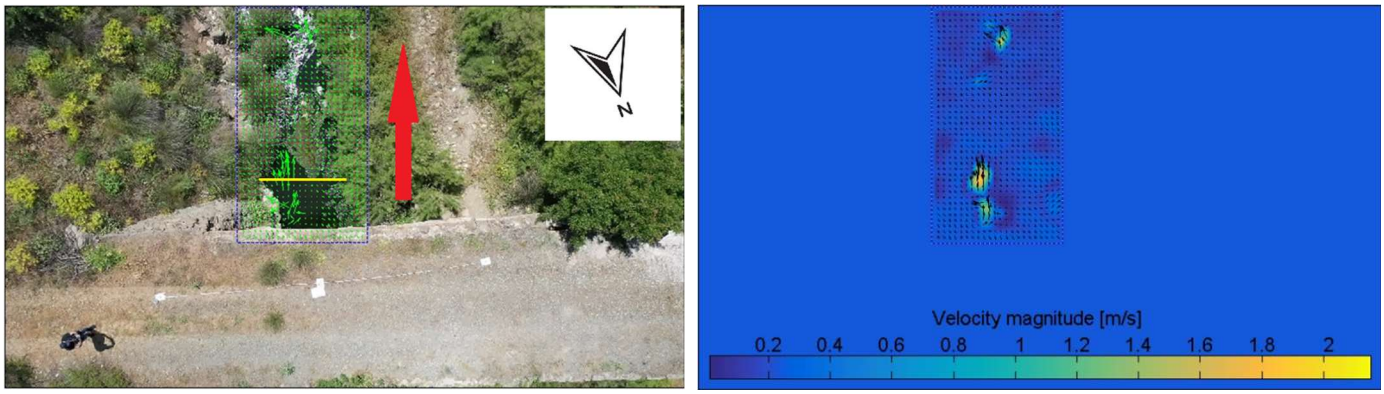

(**a**) (**b**)

Figure 3. The studied section of Agia Anna—Polichnitos captured by the UAV (**a**) the vectors of velocity are depicted in green color; (**b**) the vectors of velocity are depicted in a colorized scale where dark blue corresponds to 0 and yellow to > 2 m/s.

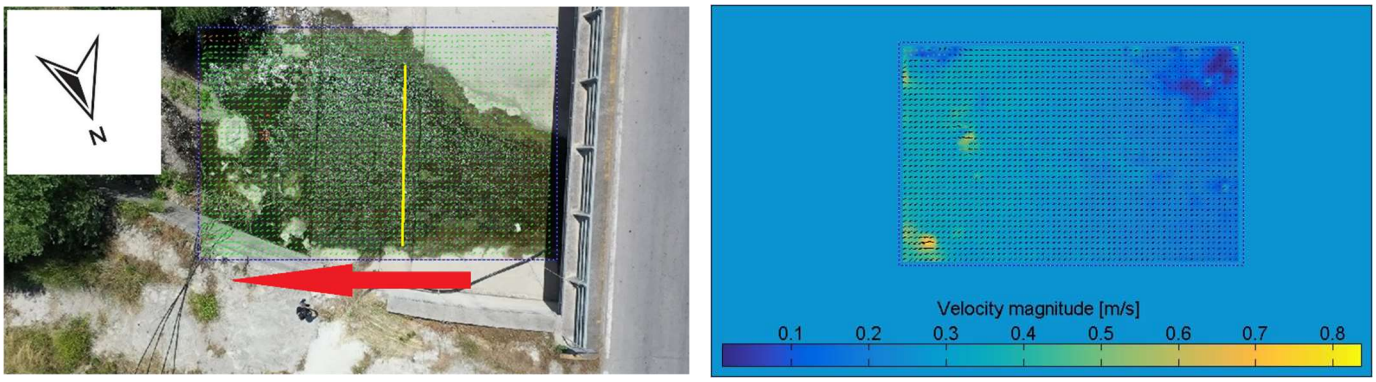

(**a**) (**b**)

Figure 4. The studied section of Kalloni captured by the UAV (**a**) the vectors of velocity are depicted in green color; (**b**) the vectors of velocity are depicted in a colorized scale where dark blue corresponds to 0 and yellow up to 0.8 m/s.

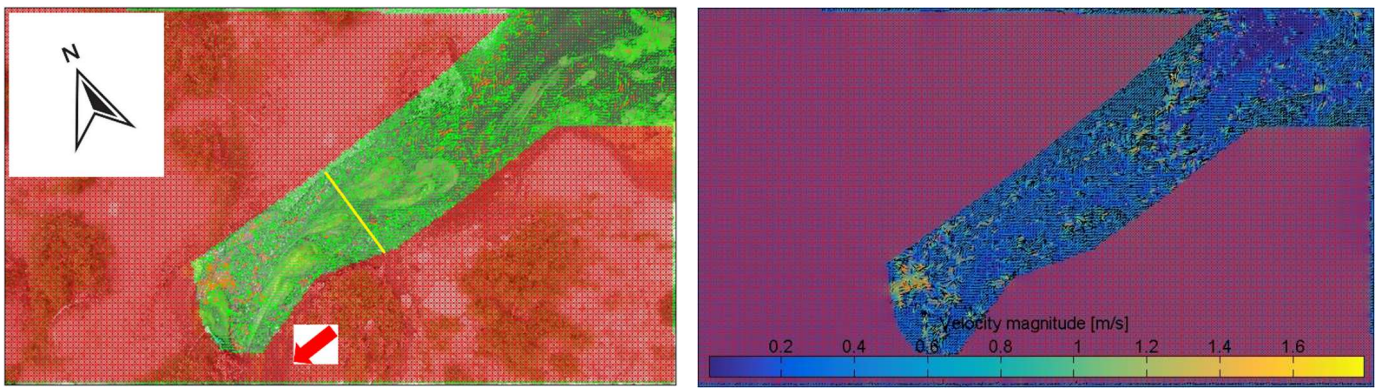

(**a**) (**b**)

Figure 5. The studied section of Evergetoulas—Kerameia captured by the UAV (**a**) the vectors of velocity are depicted in green color and the red area was excluded from analysis; (**b**) the vectors of velocity are depicted in a colorized scale where dark blue corresponds to 0 and yellow up to 1.8 m/s.

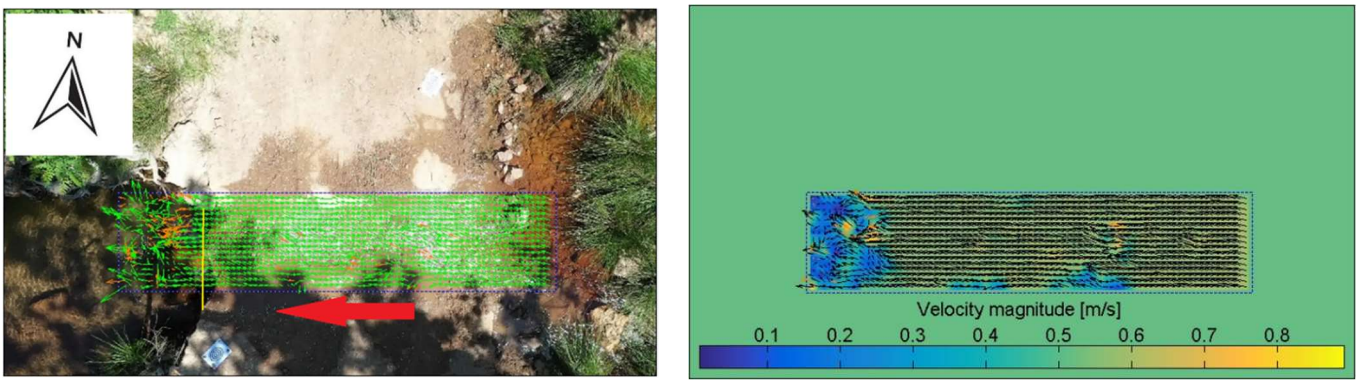

(**a**) (**b**)

Figure 6. The studied section of Pterounta—Vathilimno captured by the UAV (**a**) the vectors of velocity are depicted in green color; (**b**) the vectors of velocity are depicted in a colorized scale where dark blue corresponds to 0 and yellow to > 0.8 m/s.

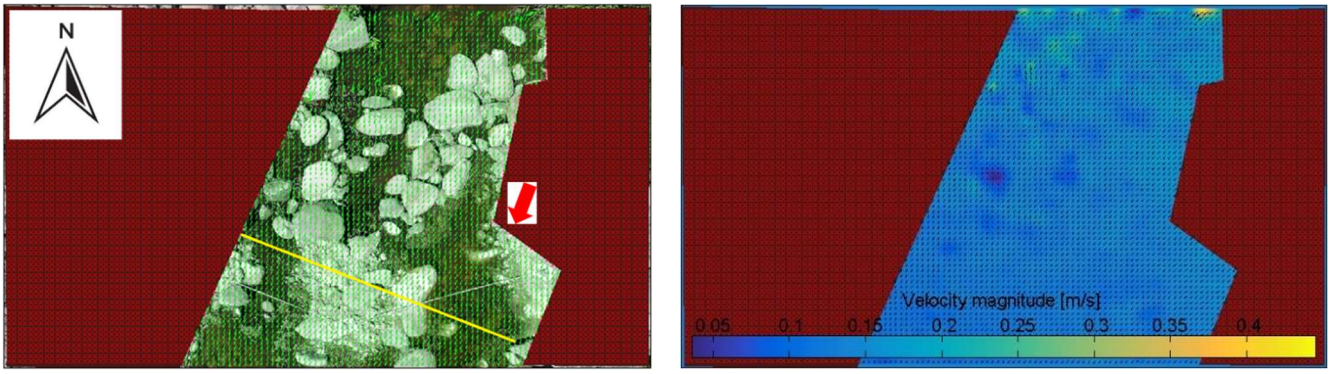

(**a**) (**b**)

Figure 7. The studied section of Eresos captured by the UAV (**a**) the vectors of velocity are depicted in green color and the red area was excluded from analysis; (**b**) the vectors of velocity are depicted in a colorized scale where dark blue corresponds to 0 and yellow up to 0.45 m/s.

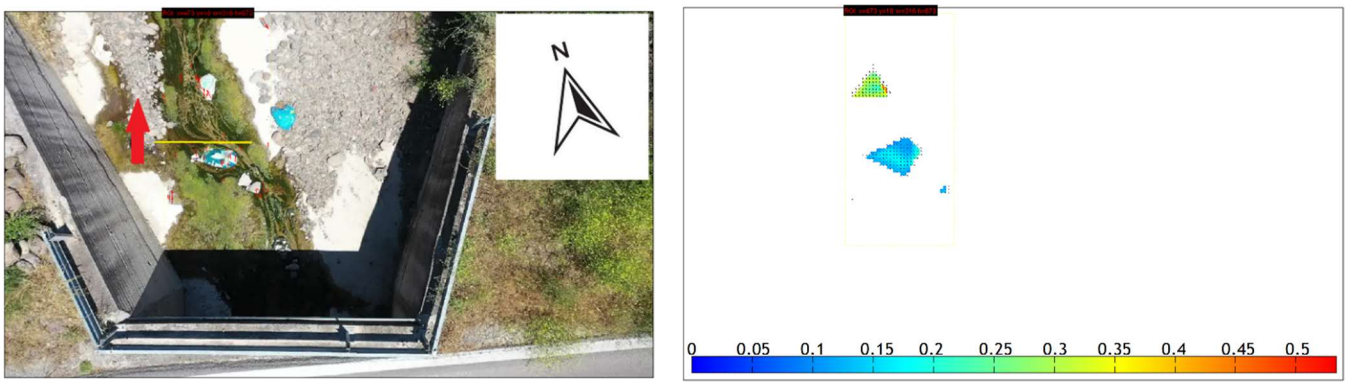

(**a**) (**b**)

Figure 8. The studied section of Agra captured by the UAV (**a**) the vectors of velocity are depicted in green color; (**b**) the vectors of velocity are depicted in a colorized scale where dark blue corresponds to 0 and yellow to >0.8 m/s.

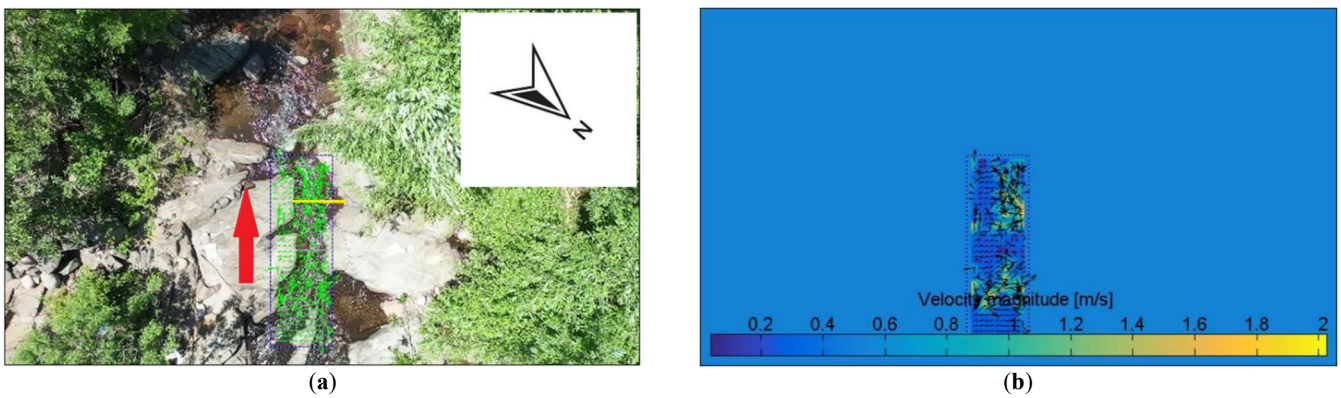

(**a**) (**b**)

Figure 9. The studied section of Kremasti Bridge—Agia Paraskevi captured by the UAV (**a**) the vectors of velocity are depicted in green color; (**b**) the vectors of velocity are depicted in a colorized scale where dark blue corresponds to 0 and yellow to 2 m/s.

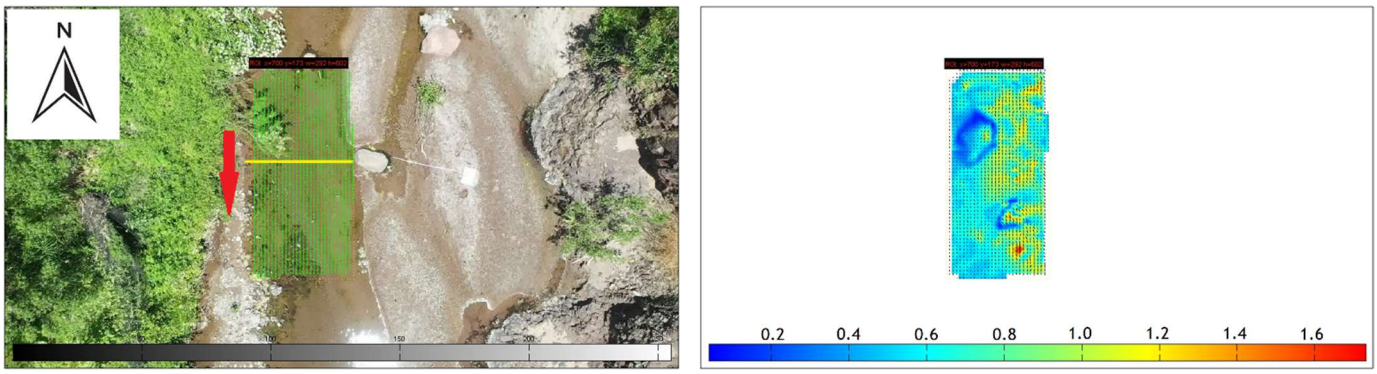

(**a**) (**b**)

Figure 10. The studied section of West of Kremasti Bridge captured by the UAV (**a**) the vectors of velocity are depicted in green color; (**b**) the vectors of velocity are depicted in a colorized scale where dark blue corresponds to 0 and yellow to > 1.8 m/s.

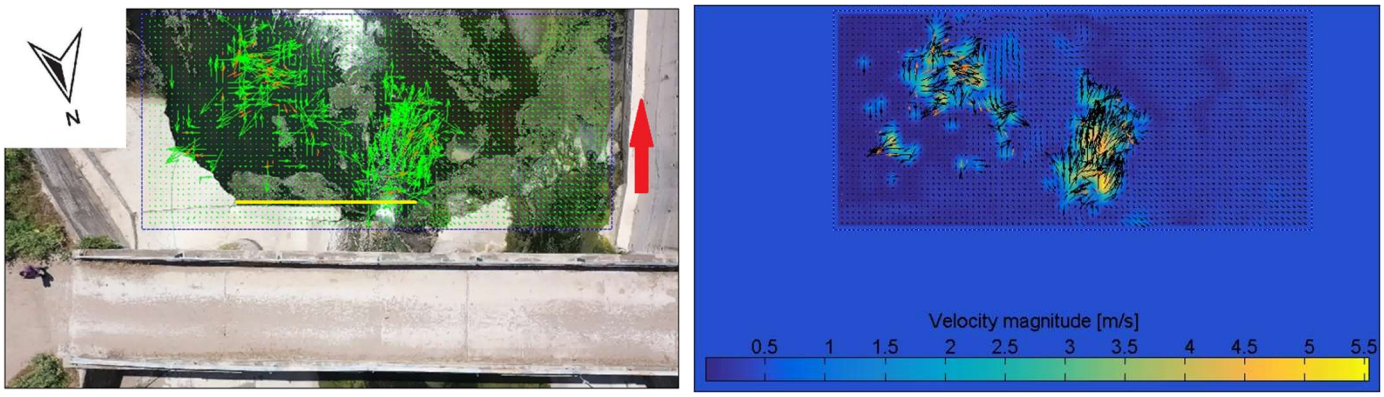

(**a**) (**b**)

Figure 11. The studied section of Prinis Bridge—Agia Paraskevi captured by the UAV (**a**) the vectors of velocity are depicted in green color; (**b**) the vectors of velocity are depicted in a colorized scale where dark blue corresponds to 0 and yellow up to 5.5 m/s.

Table 2. Results of the IV-UAV method on IRES cross sections of Lesvos Island during the dates that measurements taken.

Location (Date)	Channel Width (m)	Water Depth (m)	Surface Velocity Range (m/s)	Maximum Water Discharge (m^3/s)
Agia Anna—Polichnitos (12-5-2021)	1.50	0.05	0 to 2.0	≤0.15
Kalloni (13-5-2021)	4.00	0.02	0 to 0.8	0.07
Evergetoulas—Kerameia (15-5-2021)	3.70	0.04	0 to 1.6	0.25
Pterounta—Vathilimno (16-5-2021)	1.25	0.04	0 to 0.8	0.04
Eresos (17-5-2021)	2.50	0.09	0 to 0.4	0.09
Agra (18-5-2021)	1.30	0.03	0 to 0.5	0.02
Kremasti Bridge—Agia Paraskevi (19-5-2021)	0.60	0.28	0 to 2.0	0.34
West of Kremasti Bridge (19-5-2021)	1.50	0.035	0 to 1.6	0.08
Prinis Bridge—Agia Paraskevi (19-5-2021)	3.65	0.03	0 to 5.5	0.60

4. Discussion

Some of the areas were captured in high-altitude recordings in order to have stable ground control points in the frame, but this resulted to an analysis of very small percentage of the frames concerning the final region-of-interest. The PIVlab produced the vectors (green arrows) showing also the direction of the flow (red arrow) compared to the North symbol. As the produced vectors can be harsh to be distinguished, the surface velocity magnitude was depicted in colorized scale to help the viewer. In most cases, the streamflow is along the Y video axis, this does not affect the results; the same image would be resulted in X axis. The maximum potential flow rate estimation was done on selected cross-section representing the channel's width (yellow lines).

In the Agia Anna—Polichnitos (Figure 5), the surface velocity ranged from 0 and to >2 m/s. The velocity ratio was retrieved only in certain areas of the water surface where ripples captured and analyzed to produce the velocity's vector groups. This was done due the high altitude of the flight and due to the vegetation presence, which covered areas even in the main channel.

In the section of Kalloni's channel, the velocity was 0 to 0.8 m/s (Figure 6). The greater velocity was mainly depicted in the left side of the image where the water depth increased while the overall image showed a low velocity magnitude.

The velocity in Evergetoulas—Kerameia site ranged from 0 to 1.8 m/s (Figure 7). In the site, the surface velocity field appears to be very noisy, and it's hard to deduct if this is due to the actual surface velocities or false detections from other surface structures. The presence of vegetation is intense in the specific stream that induces errors in the velocity magnitude.

Moving on to the Pterounta—Vathilimno site (Figure 8), the surface velocity field changed suddenly and dramatically in shadowed areas of the image. The velocities increased once the stream reached a downhill area (on the left side at the edge of the forested road). Additionally, there were ripples created from the small waterfall effect as depicted by the velocity vectors in the specific small pool. But, overall, in the left side the velocity was low due to the increase of the water depth.

Next site representing the Eresos stream resulted to velocities up to 0.45 m/s. However, as depicted in Figure 9, this maximal velocity only appears in one spot at the topmost edge of the image. PIV results are known to be inaccurate in edge regions due to the reduction of neighboring data [118]. In the remaining image areas, there are no distinctions in magnitude between the water surface and on the static objects (rocks). This indicates that either the UAV video was not perfectly stable relative to the ground or the not representative of the motion of the water surface was unable to retrieved due to the underground capturing of streambed rocks. Generally, field survey recorded a very low water flow that could not produce ripples on the rocks' edges; thus, as particle size distribution has great impacts on the water turbidity [119]; a rocky streambed (boulders and cobbles) torrent with a low water depth and flow seem to arise errors in the outputs of IV-UAV.

The section in Agra was captured after the exit of a bridge. The study area had very low water level, velocity and water flow. Due to the standing waters, algae blooms covered the greater surface of the water. In addition, litter was recorded as can be seen in the image (plastic bugs). The surface velocity was able captured in limited places due to the absence or sparse distribution of floating objects. The surface velocity ranged from 0–0.3 m/s and only one location recorded up to 0.5 m/s.

In the Kremasti Bridge—Agia Paraskevi (Figure 11) a small part of the stream was captured in order to analyzed. The sun reflection on the water surface produced many unwanted vectors. In addition, windy conditions induced error due to vegetation movement and UAV instability. The tight stream had alternating directions acting as a "meandering" stream producing currents that frustrate the viewer showing a chaotic pattern of different vector's directions. Although these difficulties, the upper part of the stream showcased a satisfactory result of moving directions and estimated velocities of up to 2 m/s.

In the studied section "West of Kremasti Bridge" the velocity was greater on the right side of the main water channel and reached over 1.8 m/s. The left side was characterized by sediment deposition due to lower velocities and from vegetation presence. A branch moved by the wind was able to produce false vectors of motion on the upper left side.

The implementation at the Prinis Bridge—Agia Paraskevi site measured surface velocities up to 5.5 m/s. These velocities were recorded in a narrow location where a small waterfall is also created. As can be seen, from that point on, the water flows in a greater cross section that has also greater water depth. Additionally, PIVlab produced great velocities on the left side due to wavelike characteristics. There have been large areas over the water surface without or very low velocity data because the area acts is a small pool after a small waterfall with this limited water amounts. Furthermore, the area is covered by stable algae blooms. The sun reflection on the water surface could produce false velocities, instead it did not give any outputs.

Overall, the produced results show that the IV-UAV can be implemented at low discharges and temporary streams. Although, the measurements were performed during a period of low water level, this is the general conditions that we realize in the Greek Islands [120–121]. There are many water shortages especially in summer months when water supply mainly relies on the groundwater resources or in occasion in desalination. The described UAV-based methodology is a proven and widely utilized tool that enables us to estimate fast, accurately and safe the surface velocity on streams/river but also the water discharge in order to further develop water resources management plans. Although successful, there were many occasions that measurements were unable due to various reasons from prohibited points (e.g., prohibited areas for flights such as airports, archaeological sites, military, etc.) to areas that GPS signal was unavailable due to morphologic or vegetation issues. In these sites, only manual flights were possible but these would produce unstable video and would be also an unsafe flight. Next photos (Figure 12) present places where although water conditions were good, it was not easy (or impossible) to calculate velocity due to other difficulties. Examples can be the high and dense vegetation that blocks the water visibility. In addition, water scarcity or standing water provides limited or even no flow to be recorded. The color of the water also plays an important role and it is difficult to utilize the method in poor water quality or when siltation alters the water visibility. Furthermore, in transitional waters (areas where freshwater meets the sea, such as estuaries, deltas, and lagoons) the frequent sea wind induces surface currents in the opposite direction of water movement. Finally, the reflectance from the sun or other shadows e.g., from tree canopy introduce errors in the vectors of moving particles.

(**a**)

(**b**)

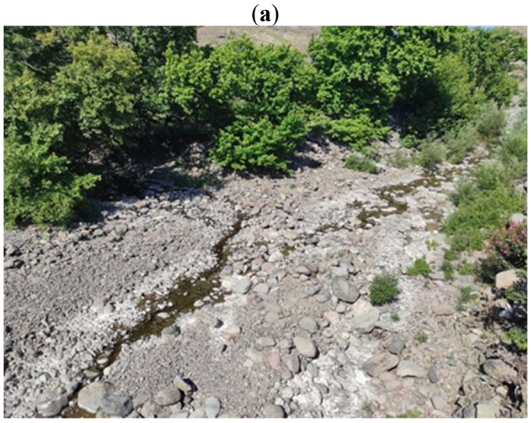

(**c**)

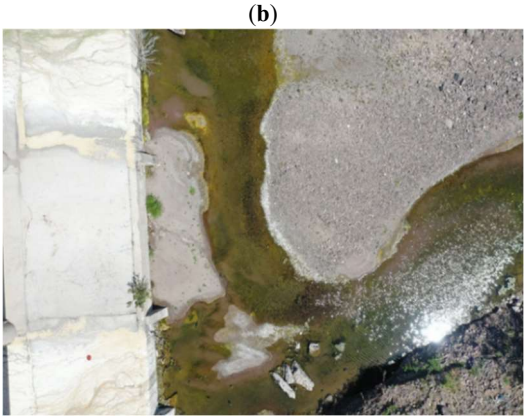

(**d**)

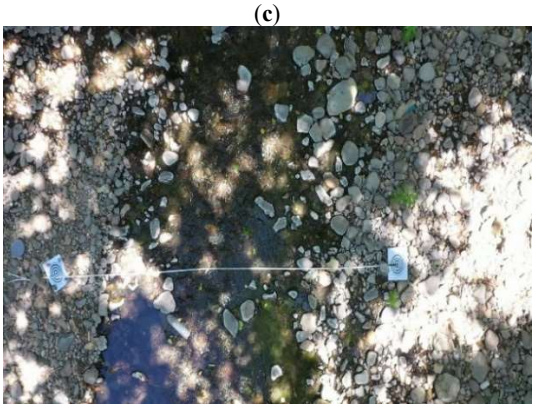

(**e**)

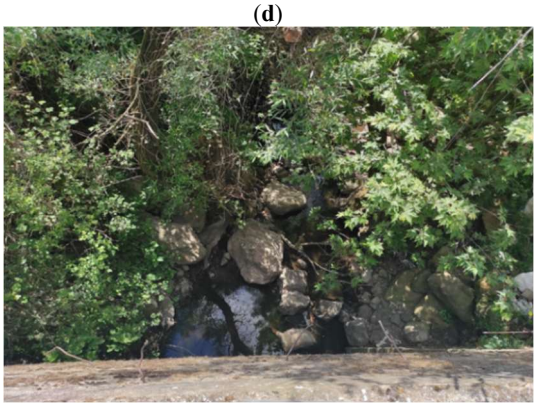

(**f**)

(**g**)

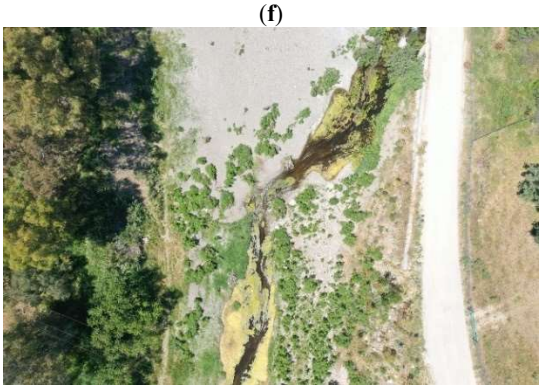

(**h**)

(**i**)

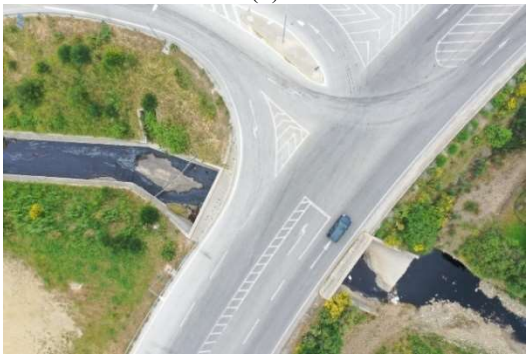

(**j**)

Figure 12. Examples of no IV-UAV implementation due to (**a**) high vegetation; (**b**) frequently in coastal areas wind creates surface waves against the real water flow; (**c**) very limited water existence, not enough width to be recorded by UAVs; (**d**) not flowing water + sun reflectance; (**e**) shadows from the tree canopy; (**f**) very limited access; (**g**) good water visibility but water quality was poor—dead animal bodies or carcasses; (**h**) good water visibility but water quality was poor - anthropogenic litter and algae bloom; (**i**) no water flow; (**j**) contaminated water—black colo—intense odor.

The ecological health of streams and rivers is evaluated and tracked using a set of established processes and recommendations known as environmental protocols. These procedures are intended to guarantee quality and consistency in the gathering and analysis of environmental data as well as to serve as a benchmark for comparing outcomes across various regions and epochs [122]. Most environmental protocols use field survey for terrestrial or aquatic monitoring to record the different environmental characteristics. Moreover, with the rapidly growing technology of UAVs existing field protocols now include also aerial and remote sensing techniques [123,124]. As for future research directions, we want to include the described methodology in optical protocols used to classify the environmental quality of the low-order streams. Flow regimes can differ during seasonal changes, depending on weather conditions and the geographical longitude or latitude that the river body covers [125,126]. Larger or smaller rivers, intermittent or perennial streams, both are studied all over the globe, with most scientists creating methods or protocols in order to standardize the way that research should be conducted for optimizing results [127]. These methods can be grouped into four categories as mentioned in [128]:

- physical habitat assessment;
- riparian habitat assessment;
- morphological assessment;
- assessment of hydrological regime alteration.

The following Table 3 presents eleven environmental protocols in which different methods of observation have been used. In several of these protocols either the entire length of the river or parts of it were studied. Each protocol suggests different variables to be studied (e.g., salinity/chemicals, morphology of channel, aquatic state, water velocity, slope, vegetation, tools, etc.) [129–139]. Some of the variables are treated with the same monitoring tools, while others differ depending on the choice of the researcher. The aquatic state (existence of water, lakes and dry riverbed) as well as the velocity/discharge and water quality/appearance seem that have not been studied thoroughly yet (especially via UAV) [140] although they are considered very important in hydrologic-ecologic studies. As a consequence, stream conditions and ecological flow monitoring are very important characteristics and the creation of a single UAV-based protocol for the environmental study of rivers is more necessary than ever [141]. This study is the first step to define the aquatic stage and water velocity via IV-UAV methodology. These are initial results in order to further incorporate the methodology in the development of a pioneer environmental UAV-based protocol to access the environmental quality of streams. The above results demonstrate the potential of UAV-based optical methods for estimating flow in temporary streams and evaluating their environmental status. These methods can provide a valuable tool for understanding the dynamics of these ecosystems and monitoring changes over time.

Table 3. Different parameters included in environmental protocols to classify the environmental status of streams.

Environmental Protocol [Reference]	[129]	[130]	[131]	[132]	[133]	[134]	[135]	[136]	[137]	[138]	[139]
Salinity/Chemical Analysis	X	X	X	X	X	X	X	√	X	√	X
Substrate	√	√	√	√	X	√	√	√	X	√	X
Vegetation	√	√	√	√	√	√	√	X	X	√	√
Land Cover/Use	√	X	√	X	√	X	√	X	X	√	√
Slope	X	V	X	X	X	X	√	√	X	√	√
Morphology	√	√	X	X	√	√	√	X	√	√	√
Flow Type	√	√	X	X	X	√	X	√	√	√	√
Aquatic STATE	X	√	X	X	X	√	X	X	X	X	X
Bathymetry	√	√	√	√	√	X	X	X	X	X	X
Water Velocity	√	√	X	√	X	√	√	X	√	√	√
Tools	Field	Field/UAV/satellite	UAV	Field/UAV	Field/UAV	Field	Field	Field	Field	Field	Field

The hydrological characteristics of Table 3 appear in scientific articles as bibliographic references or as research methods or protocol suggestions [129–139]. The majority of them refer to pieces of methodology performed in the field or with remote sensing methods, and they are mostly found in the study of intermittent, but also continuous flow rivers. Some of the characteristics identified in the chosen protocols are discussed further below. Slope, substrate, and bathymetry are crucial parameters in the study of rivers because they constitute the base of model creation as they are raw data for scientists to manage. They help a lot in the creation of mapping material. Also, they are needed as model input data in various models (InVest, SWAT, etc.) for water quality purposes. They play a significant role in shaping the physical, chemical, and biological conditions of river ecosystems. The slope of a river determines its flow velocity which the physical characteristics of the river such as its channel morphology, sediment transport, and water depth. Steeper slopes are associated with faster flow rates and shorter travel times between different parts of the river system. The substrate of a river refers to the material on the riverbed, which can include rocks, gravel, sand, and mud. The

substrate is crucial for understanding the physical and chemical parameters of the river because it influences water quality, nutrient cycling, and aquatic life habitat availability. Bathymetry is the measuring of water depth in a river, which is vital for understanding physical river properties such as channel form, flow velocity, and sediment transport.

In environmental regulations, vegetation is an important indicator for classifying the environmental state of streams. Vegetation can reveal the stream's physical, chemical, and biological characteristics, as well as its ecological roles and services [142–144]. Riparian vegetation is the vegetation that grows along the banks of a stream and plays an important part in the stream's ecological health [145]. Riparian vegetation assessment protocols may identify; the species composition, estimating the width of the riparian zone, and assessing the vegetation cover. Aquatic invertebrates are key markers of stream health and can be used to evaluate the influence of human activities on stream ecosystems [146]. Protocols for aquatic invertebrate evaluation may determine the number, diversity, and species composition of invertebrates in the stream. Macrophytes are freshwater plants that grow in stream channels and can be utilized to assess water quality and environmental health [147]. Macrophyte evaluation techniques may involve measurements of macrophyte abundance, diversity, and species composition in the stream.

Flow type patterns in intermittent rivers can vary depending on the season and weather conditions. During the rainy season, some intermittent rivers may experience high flows, while others may experience only episodic flow. Most protocols detect the flow types by field research rather than remote sensing techniques. The following methods are suggested to monitor the flow patterns of intermittent rivers [148–150]:

- Flow measurement: Install a flow measurement system to determine the river's flow rate. This can be accomplished using a variety of tools, such as current meters, acoustic Doppler current profilers, and flow gauges;
- Flow duration: Calculate the length of the river that is flowing at different times, as well as the duration of flow events and dry periods;
- Flow timing: Keep track of the timing of flow events, such as the onset and cessation of flow;

Land use and land cover are two distinct but related concepts that describe how land is used and the physical characteristics of its surface. Land use refers to how humans use land, such as agricultural land, residential areas, industrial areas, or protected areas such as parks and reserves. It describes human activities on the land, as well as how it is managed and transformed for various purposes. In contrast, land cover refers to the physical characteristics of the land surface, such as vegetation, water bodies, soil type, and natural features such as mountains and valleys. It describes the land's natural and physical characteristics, as well as how they contribute to the environment. Land use and land cover are related but not the same thing. Natural processes and features determine land cover, whereas human activities and management decisions influence land use. A forest area, for example, could have the same land cover but different land uses such as timber production, recreation, or conservation. Land use refers to how humans use and manage land, whereas land cover refers to the physical characteristics of the land surface [151]. The above protocols detect the land cover for modeling purposes, and they discuss the land usage in their conclusions concerning human activity.

The aquatic state is a term used in environmental regulations to describe the state and quality of water resources in a particular ecosystem, including rivers, lakes, wetlands, and coastal areas. Water chemistry, physical habitat characteristics, aquatic biota, and ecosystem processes are used to determine the aquatic status. The aquatic condition is a critical indicator for assessing aquatic ecosystem health and recognizing potential risks to their integrity [152]. The goal of aquatic environmental protocols is to develop rules and standards for water quality and management techniques in order to maintain or improve the ecological health of aquatic ecosystems.

5. Conclusions

Temporary streams are an important component of the hydrological cycle in arid and semi-arid regions, but their flow is highly variable and difficult to quantify due to their intermittent character. Conventional flow measurement tools, like as current meters and stream gauges, might be difficult to utilize in these conditions. Unmanned aerial vehicles (UAVs) offer a promising alternative for measuring flow in temporary streams.

Climate change, physical and biological changes, and anthropogenic litter, particularly macro and micro-plastic pollution, make IRES vulnerable. Monitoring, evaluating, and categorizing their environmental status is critical. Recent advances in photogrammetry and image-based velocimetry monitoring techniques hold considerable promise for IRES monitoring, allowing for low-cost real-time observations with excellent spatial resolution. Natural river monitoring techniques, such as IV-UAV, are frequently employed, and they involve tracer seeding and picture recording.

In conclusion, accurate river discharge data is crucial for hydrological processes and various practical applications, especially in arid or semi-arid regions where flash flood warning systems are limited. As discussed above, the successful implementation of IV-UAV methodology on different IRES cross-sections in Lesvos Island using the simple RGB camera of the UAV platform resulted in a good water visibility pattern in all case studies except for one cross section where the depth was higher and water was flowing. Fauna was also recorded in some cases. Overall, this methodology could be incorporated in UAV-based optical protocols. This would help estimating flow in IRES and evaluating their environmental status quick, safe and easy.

Appendix

Table A1. The studied cross sections at IRES of Lesvos Island.

Location (Cross-section)	Date	X	Y	Z	UAV Height	Water Conditions
Agia Anna—Polichnitos	12-5-2021	39°03′28.8″ N	26°11′34.8″ E	28.0	20	good visibility—flowing water—shallow depth
Kalloni	13-5-2021	39°12′16.9″ N	26°10′39.4″ E	8.40	10	good visibility—flowing water—shallow depth
Evergetoulas—Kerameia	15-5-2021	39°07′43.7″ N	26°25′35.1″ E	44.30	10	good visibility—flowing water—shallow depth
Pterounta—Vathilimno	16-5-2021	39°12′41.6″ N	26°03′06.5″ E	238.01	5	good visibility—flowing water—shallow depth
Eresos	17-5-2021	39°08′38.3″ N	25°59′14.0″ E	74.39	7	good visibility—flowing water—shallow depth
Agra	18-5-2021	39°09′0.18″ N	26°04′20.12″ E	185.86	10	good visibility—flowing water—shallow depth
Kremasti Bridge—Agia Paraskevi	19-5-2021	39°16′13.3″ N	26°15′10.5″ E	70.34	15	good visibility—flowing water—shallow depth
West of Kremasti Bridge	19-5-2021	39°16′29.0″ N	26°14′38.4″ E	66.21	20	good visibility—flowing water—shallow depth
Prinis Bridge—Agia Paraskevi	19-5-2021	39°15′10.1″ N	26°15′05.0″ E	44.03	30	low visibility—flowing water—significant depth

Author Contributions

Conceptualization, P.K. and O.T.; methodology, P.K.; software, P.K.; validation, P.K., M.-D.S.; writing—original draft preparation, P.K.; writing—review and editing, O.T.; visualization, P.K. and M.-D.S.; supervision, O.T. All authors have read and agreed to the published version of the manuscript.

Funding

This research received no external funding.

Declaration of Competing Interest

The authors declare that they have no known competing financial interests or personal relationships that could have appeared to influence the work reported in this paper.

References

1. Pumo D, Lo Conti F, Viola F, Noto LV. An automatic tool for reconstructing monthly time-series of hydro-climatic variables at ungauged basins. Environ. *Model. Softw.* **2017**, *95*, 381–400.
2. Stein R, Dittmers K, Fahl K, Kraus M, Matthiessen J, Niessen F, Fütterer DK. Arctic (palaeo) river discharge and environmental change: evidence from the Holocene Kara Sea sedimentary record. *Quat. Sci. Rev.* **2004**, *23*, 1485–1511.
3. Auble GT, Friedman JM, Scott ML. Relating riparian vegetation to present and future streamflows. *Ecol. Appl.* **1994**, *4*, 544–554.
4. Zaimes GN, Schultz RC, Isenhart TM. Riparian land uses and precipitation influences on stream bank erosion in Central IOWA. *J. Am. Water Resour. Assoc.* **2006**, *42*, 83–97.
5. Al-Mamari MM, Kantoush SA, Kobayashi S, Sumi T, Saber M. Real-time measurement of flash-flood in a Wadi Area by LSPIV and STIV. *Hydrology* **2019**, *6*, 27.
6. Stamataki MD, Tzoraki O, Sauqeut E. Time-lapse graphical representation methods for mapping of Intermittent Rivers and Ephemeral Streams (IRES). *Eur. J. Geogr.* **2021**, *12*, 51–67.
7. Martin J, Kurc SA, Zaimes G, Crimmins M, Hutmacher A, Green D. Elevated air temperatures in riparian ecosystems along ephemeral streams: The role of housing density. *J. Arid. Environ.* **2012**, *84*, 9–18.
8. Datry T, Singer G, Sauquet E, Capdevilla DJ, Von Schiller D, Subbington R, et al. Science and management of intermittent rivers and ephemeral streams (SMIRES). *Res. Ideas Outcomes* **2017**, *3*, 1–23.
9. Nabih S, Tzoraki O, Zanis P, Tsikerdekis T, Akritidis D, Kontogeorgos I, et al. Alteration of the Ecohydrological Status of the Intermittent Flow Rivers and Ephemeral Streams due to the Climate Change Impact (Case Study: Tsiknias River). *Hydrology* **2021**, *8*, 43.
10. Tzoraki O, Amaxidis Y, Skoulikidis NT, Nikolaidis NP. In-Stream Geochemical Processes of Temporary Rivers—Krathis River Case Study. In Proceedings of the Restoration and Protection of the Environment VII Conference, Mykonos, Greece, 28 June–1 July 2004.
11. Tramblay Y, Rutkowska A, Sauquet E, Sefton C, Laaha G, Osuch M, et al. Trends in flow intermittence for European rivers. *Hydrol. Sci. J.* **2021**, *66*, 37–49.
12. A Catalogue of European Intermittent Rivers and Ephemeral Streams. Available online: https://hal.archives-ouvertes.fr/hal-02914572/file/Sauquet_et_al_2020Catalogue_SMIRES.pdf (accessed on 5 August 2022).
13. Tzoraki O, Nikolaidis NP, Amaxidis Y, Skoulikidis NT. In-stream biogeochemical processes of a temporary river. *Environ. Sci. Technol.* **2007**, *41*, 1225–1231.
14. Tzoraki O, Nikolaidis NP. A generalized framework for modeling the hydrologic and biogeochemical response of a Mediterranean temporary river basin. *J. Hydrol.* **2007**, *346*, 112–121.
15. Garcia C, Amengual A, Homar V, Zamora A. Losing water in temporary streams on a Mediterranean island: Effects of climate and land-cover changes. *Glob. Planet Change* **2017**, *148*, 139–152.

16. Tzoraki O. Operating small hydropower plants in Greece under intermittent flow uncertainty: The case of Tsiknias River (Lesvos). *Challenges* **2020**, *11*, 17.
17. Myronidis D, Nikolaos T. Changes in climatic patterns and tourism and their concomitant effect on drinking water transfers into the region of South Aegean, Greece. *Stoch. Environ. Res. Risk Assess*. **2021**, *35*, 1725–1739.
18. Stathi E, Kastridis A, Myronidis D. Analysis of Hydrometeorological Trends and Drought Severity in Water-Demanding Mediterranean Islands under Climate Change Conditions. *Climate* **2023**, *11*, 106.
19. Costigan KH, Kennard MJ, Leigh C, Sauquet E, Datry T, Boulton AJ. Flow Regimes in Intermittent Rivers and Ephemeral Streams. In *Intermittent Rivers and Ephemeral Streams*; Academic Press: Cambridge, MA, USA, 2017.
20. Gutiérrez-Jurado KY, Partington D, Batelaan O, Cook P, Shanafield M. What triggers streamflow for intermittent rivers and ephemeral streams in low-gradient catchments in Mediterranean climates. *Water Resour. Res.* **2019**, *55*, 9926–9946.
21. Boulton AJ, Rolls RJ, Jaeger KL, Datry T. Hydrological connectivity in intermittent rivers and ephemeral streams. In *Intermittent Rivers and Ephemeral Streams*; Academic Press: Cambridge, MA, USA, 2017.
22. Datry T, Boulton AJ, Bonada N, Fritz K, Leigh C, Sauquet E, et al. Flow intermittence and ecosystem services in rivers of the Anthropocene. *J. Appl. Ecol.* **2018**, *55*, 353–364.
23. Chiu MC, Leigh C, Mazor R, Cid N, Resh V. Anthropogenic threats to intermittent rivers and ephemeral streams. In *Intermittent Rivers and Ephemeral Streams*; Academic Press: Cambridge, MA, USA, 2017.
24. Aslam S, Tzoraki O, Krasakopoulou E. Anthropogenic litter in freshwater bodies and their estuaries: an empirical analysis in Lesvos, Greece. *Environ. Sci. Pollut. Res.* **2021**, *29*, 1–13.
25. Brownson RC, Hoehner CM, Day K, Forsyth A, Sallis JF. Measuring the built environment for physical activity: State of the science. *Am. J. Prev. Med.* **2009**, *36*, S99–S123.
26. Sallis J, Bauman A, Pratt M. Environmental and policy interventions to promote physical activity. *Am. J. Prev. Med.* **1998**, *15,* 379–397.
27. De'ath G. Fabricius KE. Classification and regression trees: A powerful yet simple technique for ecological data analysis. *Ecology* **2000**, *81*, 3178–3192.
28. Moretti M, Dias AT, De Bello F, Altermatt F, Chown SL, Azcárate FM, et al. Handbook of protocols for standardized measurement of terrestrial invertebrate functional traits. *Funct. Ecol.* **2017**, *31*, 558–567.
29. Qureshi A, Badola R, Hussain SA. A review of protocols used for assessment of carbon stock in forested landscapes. *Environ. Sci. Policy* **2012**, *16*, 81–89.
30. Forsyth A, Schmitz KH, Oakes M, Zimmerman J, Koepp J. Standards for environmental measurement using GIS: Toward a protocol for protocols. *J. Phys. Act. Health* **2006**, *3*, S241–S257.
31. Tmušić G, Manfreda S, Aasen H, James MR, Gonçalves G, Ben-Dor E, et al. Current practices in UAS-based environmental monitoring. *Remote Sens.* **2020**, *12*, 1001.
32. Singhal G, Bansod B, Mathew L. Unmanned aerial vehicle classification, applications and challenges: A review. *Preprints* **2018**. doi:10.20944/preprints201811.0601.v1.
33. Seier G, Hödl C, Abermann J, Schöttl S, Maringer A, Hofstadler DN, et al. Unmanned aircraft systems for protected areas: Gadgetry or necessity? *J. Nat. Conserv.* **2021**, *64*, 126078.
34. Fallati L, Polidori A, Salvatore C, Saponari L, Savini A, Galli P. Anthropogenic Marine Debris assessment with Unmanned Aerial Vehicle imagery and deep learning: A case study along the beaches of the Republic of Maldives. *Sci. Total Environ.* **2019**, *693*, 133581.
35. Hughes M, Hornby DD, Bennion H, Kernan M, Hilton J, Phillips G, et al. The development of a GIS-based inventory of standing waters in Great Britain together with a risk-based prioritisation protocol. *Water Air Soil Pollut.* **2004**, *4*, 73–84.
36. Doukari M, Batsaris M, Papakonstantinou A, Topouzelis K. A protocol for aerial survey in coastal areas using UAS. *Remote Sens.* **2019**, *11*, 1913.
37. Rivas Casado M, Ballesteros Gonzalez R, Kriechbaumer T, Veal A. Automated identification of river hydromorphological features using UAV high resolution aerial imagery. *Sensors* **2015**, *15*, 27969–27989.
38. Lane SN, Gentile A, Goldenschue L. Combining UAV-based SfM-MVS photogrammetry with conventional monitoring to set environmental flows: modifying dam flushing flows to improve alpine stream habitat. *Remote Sens*. **2020**, *12*, 3868.
39. Manfreda S, Dor EB. Remote sensing of the environment using unmanned aerial systems. In *Unmanned Aerial Systems for Monitoring Soil, Vegetation, and Riverine Environments*; Elsevier: Amsterdam, The Netherlands, 2023.
40. Gray PC, Windle AE, Dale J, Savelyev IB, Johnson ZI, Silsbe GM, et al. Robust ocean color from drones: Viewing geometry, sky reflection removal, uncertainty analysis, and a survey of the Gulf Stream front. *Limnol. Oceanogr. Methods* **2022**, *20*, 656–673.
41. Dimitriou E, Stavroulaki E. Assessment of riverine morphology and habitat regime using unmanned aerial vehicles in a Mediterranean environment. *Pure Appl. Geophys.* **2018**, *175*, 3247–3261.
42. De Keukelaere L, Moelans R, Knaeps E, Sterckx S, Reusen I, De Munck D, et al. Airborne Drones for Water Quality Mapping in Inland, Transitional and Coastal Waters—MapEO Water Data Processing and Validation. *Remote Sens.* **2023**, *15*, 1345.
43. Islam MT, Yoshida K, Nishiyama S, Sakai K, Adachi S, Pan S. Promises and uncertainties in remotely sensed riverine hydro-environmental attributes: Field testing of novel approaches to unmanned aerial vehicle-borne lidar and imaging velocimetry. *River Res. Appl.* **2022**, *38*, 1757–1774.

44. Román A, Tovar-Sánchez A, Gauci A, Deidun A, Caballero I, Colica E, et al. Water-Quality Monitoring with a UAV-Mounted Multispectral Camera in Coastal Waters. *Remote Sens.* **2022**, *15*, 237.
45. Windle AE, Silsbe GM. Evaluation of unoccupied aircraft system (UAS) remote sensing reflectance retrievals for water quality monitoring in coastal waters. *Front. Environ. Sci.* **2021**, *9*, 674247.
46. Borg Galea A, Sadler JP, Hannah DM, Datry T, Dugdale SJ. Mediterranean intermittent rivers and ephemeral streams: Challenges in monitoring complexity. *Ecohydrology* **2019**, *12*, e2149.
47. Tauro F, Piscopia R, Grimaldi S. Streamflow observations from cameras: Large-scale particle image velocimetry or particle tracking velocimetry? *Water Resour. Res.* **2017**, *53*, 10374–10394.
48. Kim Y, Muste M, Hauet A, Krajewski WF, Kruger A, Bradley A. Stream discharge using mobile large-scale particle image velocimetry: A proof of concept. *Water Resour. Res.* **2008**, *44*, 1–6.
49. Tauro F, Petroselli A, Grimaldi S. Optical sensing for stream flow observations: A review. *J. Agric. Eng.* **2018**, *49*, 199–206.
50. Manfreda S, McCabe MF, Miller PE, Lucas R, Pajuelo Madrigal V, Mallinis G, et al. On the use of unmanned aerial systems for environmental monitoring. *Remote Sens.* **2018**, *10*, 641.
51. Koutalakis P, Tzoraki O, Zaimes GN. Software utilized for image-based velocimetry methods focused on water resources. *Desalin. Water Treat.* **2021**, *218*, 1–17.
52. Muste M, Fujita I, Hauet A. Large-scale particle image velocimetry for measurements in riverine environments. *Water Resour. Res.* **2008**, *44*, 1–14.
53. Bechle AJ, Wu CH, Liu WC, Kimura N. Development and application of an automated river-estuary discharge imaging system. *J. Hydraul. Eng.* **2012**, *138*, 327–339.
54. Dramais G, Le Coz J, Camenen B, Hauet A. Advantages of a mobile LSPIV method for measuring flood discharges and improving stage–discharge curves. *J. Hydro-Environ. Res.* **2011**, *5*, 301–312.
55. Rozos E, Dimitriadis P, Mazi K, Lykoudis S, Koussis A. On the Uncertainty of the Image Velocimetry Method Parameters. *Hydrology* **2020**, *7*, 65.
56. Gleason CJ, Durand MT. Remote sensing of river discharge: A review and a framing for the discipline. *Remote Sens.* **2020**, *12*, 1107.
57. Zhu X, Lipeme Kouyi G. An analysis of LSPIV-based surface velocity measurement techniques for stormwater detention basin management. *Water Resour. Res.* **2019**, *55*, 888–903.
58. Fujita I, Muste M, Kruger A. Large-scale particle image velocimetry for flow analysis in hydraulic engineering applications. *J. Hydraul. Res.* **1998**, *36*, 397–414.
59. Tauro F, Petroselli A, Arcangeletti E. Assessment of drone-based surface flow observations. *Hydrol. Process.* **2016**, *30*, 1114–1130.
60. Perks MT, Fortunato Dal Sasso S, Hauet A, Jamieson E, Le Coz J, Pearce S, et al. Towards harmonisation of image velocimetry techniques for river surface velocity observations. *Earth Syst. Sci. Data* **2020**, *12*, 1545–1559.
61. Han X, Chen K, Zhong Q, Chen Q, Wang F, Li D. Two-Dimensional Space-Time Image Velocimetry for Surface Flow Field of Mountain Rivers Based on UAV Video. *Front. Earth Sci.* **2021**, *9*, 686636.
62. Raffel M, Willert CE, Scarano F, Kähler C, Wereley S, Kompenhans J. *Particle Image Velocimetry: A Practical Guide*; Springer International Publishing: Cham, Switzerland, 2018.
63. Patalano A, Garcia CM, Brevis W, Bleninger T, Guillen N, Moreno L, et al. Recent advances in Eulerian and Lagragian large-scale particle image velocimetry. In Proceedings of the 36th IAHR World Congress, The Hauge, Netherlands, 28 June–3 July 2015.
64. Gollin D, Brevis W, Bowman ET, Shepley P. Performance of PIV and PTV for granular flow measurements. *Granul. Matter.* **2017**, *19*, 1–18.
65. Fujita I, Watanabe H, Tsubaki R. Development of a non-intrusive and efficient flow monitoring technique: The space-time image velocimetry (STIV). *Int. J. River Basin Manag.* **2007**, *5*, 105–114.
66. Yu K, Kim S, Kim D. Correlation analysis of spatio-temporal images for estimating two-dimensional flow velocity field in a rotating flow condition. *J. Hydrol.* **2015**, *529*, 1810–1822.
67. Cameron SM. PIV algorithms for open-channel turbulence research: Accuracy, resolution and limitations. *J. Hydro-Environ. Res.* **2011**, *5*, 247–262.
68. Tauro F. Particle tracers and image analysis for surface flow observations. *Wiley Interdiscip. Rev. Water* **2016**, *3*, 25–39.
69. Muste M, Xiong Z, Bradley A, Kruger A. Large-Scale Particle Image Velocimetry–a reliable tool for physical modeling. In Proceedings of the ASCE 2000 Joint Conference on Water Resources Engineering and Water Resources Planning & Management, Minneapolis, MN, USA, 30 July–2 August 2000.
70. Koutalakis P, Zaimes GN. River Flow Measurements Utilizing UAV-Based Surface Velocimetry and Bathymetry Coupled with Sonar. *Hydrology* **2022**, *9*, 148.
71. Huang WC, Young CC, Liu WC. Application of an automated discharge imaging system and LSPIV during typhoon events in Taiwan. *Water* **2018**, *10*, 280.
72. Herzog A, Stahl K, Blauhut V, Weiler M. Measuring zero water level in stream reaches: A comparison of an image-based versus a conventional method. *Hydrol. Process.* **2022**, *36*, e14658.
73. Guillén NF, Patalano A, García CM, Bertoni JC. Use of LSPIV in assessing urban flash flood vulnerability. *Nat. Hazards* **2017**, *87*, 383–394.
74. Perks MT, Russell AJ, Large AR. Advances in flash flood monitoring using unmanned aerial vehicles (UAVs). *Hydrol. Earth Syst. Sci. Discuss*. **2016**, *20*, 4005–4015.

75. Tauro F, Porfiri M, Grimaldi S. Surface flow measurements from drones. *J. Hydrol.* **2016**, *540*, 240–245.
76. Detert M, Weitbrecht V. A low-cost airborne velocimetry system: Proof of concept. *J. Hydraul. Res.* **2015**, *53*, 532–539.
77. Lewis QW, Rhoads BL. LSPIV measurements of two-dimensional flow structure in streams using small unmanned aerial systems: 1. Accuracy assessment based on comparison with stationary camera platforms and in-stream velocity measurements. *Water Resour. Res.* **2018**, *54*, 8000–8018.
78. Unsworth CA. Particle Image Velocimetry. In *Geomorphological Techniques*; British Society for Geomorphology: London, UK, 1900.
79. Cristo C. Particle Imaging Velocimetry and its applications in hydraulics: A state-of-the-art review. In *Experimental Methods in Hydraulic Research. Geoplanet: Earth and Planetary Sciences*; Springer: Berlin/Heidelberg, Germany, 2011.
80. Koutalakis P, Tzoraki O, Zaimes GN. UAVs To Enhance Watershed Management. Examples From North Greece. In Proceedings of the 7th International Conference on Civil Protection & New Technologies "SAFE GREECE 2020", Athens, Greece, 14–16 October 2020.
81. Liu WC, Lu CH, Huang WC. Large-scale particle image velocimetry to measure streamflow from videos recorded from unmanned aerial vehicle and fixed imaging system. *Remote Sens.* **2021**, *13*, 2661.
82. Ran QH, Li W, Liao Q, Tang HL, Wang MY. Application of an automated LSPIV system in a mountainous stream for continuous flood flow measurements. *Hydrol. Process*. **2016**, *30*, 3014–3029.
83. Fovet O, Belemtougri A, Boithias L, Braud I, Charlier JB, Cottet M, et al. Intermittent rivers and ephemeral streams: Perspectives for critical zone science and research on socio-ecosystems. *Wiley Interdiscip. Rev. Water* **2021**, *8*, e1523.
84. Le Boursicaud R, Pénard L, Hauet A, Thollet F, Le Coz J. Gauging extreme floods on YouTube: Application of LSPIV to home movies for the post-event determination of stream discharges. *Hydrol. Process.* **2016**, *30*, 90–105.
85. Theule JI, Crema S, Marchi L, Cavalli M, Comiti F. Exploiting LSPIV to assess debris-flow velocities in the field. *Nat. Hazards Earth Syst. Sci.* **2018**, *18*, 1–13.
86. Thumser P, Haas C, Tuhtan JA, Fuentes-Pérez JF, Toming G. RAPTOR-UAV: Real-time particle tracking in rivers using an unmanned aerial vehicle. *Earth Surf. Process. Landf.* **2017**, *42*, 2439–2446.
87. Lewis QW, Lindroth EM, Rhoads BL. Integrating unmanned aerial systems and LSPIV for rapid, cost-effective stream gauging. *J. Hydrol.* **2018**, *560*, 230–246.
88. Mizerakis V, Strachinis I. New record of *Tarentola mauritanica* (squamata: *Phyllodactylidae*) from Lesvos Island, Greece. *Herpetol. Notes* **2017**, *10*, 157–159.
89. Hellenic Statistical Authority—2011 Population-Housing Census. Available online: https://www.statistics.gr/en/2011-census-pop-hous (accessed on 20 November 2021).
90. Tsartas P, Kyriakaki A, Stavrinoudis T, Despotaki G, Doumi M, Sarantakou E, et al. Refugees and tourism: A case study from the islands of Chios and Lesvos, Greece. *Curr. Issues Tour.* **2020**, *23*, 1311–1327.
91. Verentzioti A, Stranjalis G, Kalamatianos T, Siatouni A, Sakas DE, Gatzonis S. Epidemiology of first epileptic seizures in the northern Aegean Island of Lesvos, Greece. *Clin. Pract.* **2017**, *7,* 84–87.
92. Zouros N, Mc Keever P. The European geoparks network. *Episodes* **2004**, *27*, 165–171.
93. Margaroni SG, Tzoraki O, Velegrakis A. Soil erosion risk of Lesvos Island. In Proceedings of the 11th Panhellenic Symposium on Oceanography and Fisheries, Mytilene, Lesvos, Greece, 13–17 May 2015.
94. Papadopoulou A, Dikou A, Papapanagiotou V. A contribution to Cumulative Effects Assessment for regional sustainable development-the case of Panagiouda-Pamfilla bay, Lesvos Island, Greece. *Transit. Waters Bull.* **2014**, *8*, 53–72.
95. Karavitis CA, Kerkides P. Estimation of the water resources potential in the island system of the Aegean Archipelago, Greece. *Water Int.* **2002**, *27*, 243–254.
96. Simha P, Mutiara ZZ, Gaganis P. Vulnerability assessment of water resources and adaptive management approach for Lesvos Island, Greece. *Sustain. Water Resour. Manag.* **2017**, *3*, 283–295.
97. The DJI Mavic 2 Pro specifications. Available online: https://www.dji.com (accessed on 15 November 2021).
98. Kantoush SA, Schleiss AJ. Large-scale PIV surface flow measurements in shallow basins with different geometries. *J. Vis.* **2009**, *12*, 361–373.
99. Fang W, Zheng L. Distortion correction modeling method for zoom lens cameras with bundle adjustment. *J. Opt. Soc. Korea* **2016**, *20*, 140–149.
100. Johnson BG. Recommendations for a system to photograph core segments and create stitched images of complete cores. *J. Paleolimnol.* **2015**, *53*, 437–444.
101. Bååth H, Gällerspång A, Hallsby G, Lundström A, Löfgren P, Nilsson M, et al. Remote sensing, field survey, and long-term forecasting: an efficient combination for local assessments of forest fuels. *Biomass Bioenergy* **2002**, *22*, 145–157.
102. Parker SCJ, Hickman DL, Smith MI. Real-time processing of dual band HD video for maintaining operational effectiveness in degraded visual environments. In Proceedings of the SPIE 9471, Degraded Visual Environments: Enhanced, Synthetic, and External Vision Solutions, Baltimore, MD, USA, 21 May 2015.
103. Thielicke W, Stamhuis E. PIVlab–towards user-friendly, affordable and accurate digital particle image velocimetry in MATLAB. *J. Open Res. Softw.* **2014**, *2*, 1–10.
104. Thielicke W. The flapping flight of birds: Analysis and application. PhD Thesis, University of Groningen, Groningen, The Netherlands, 31 October 2014.
105. Kinzel PJ, Legleiter CJ. sUAS-based remote sensing of river discharge using thermal particle image velocimetry and bathymetric lidar. *Remote Sens.* **2019**, *11*, 2317.

106. Legleiter CJ, Kinzel PJ, Nelson JM. Remote measurement of river discharge using thermal particle image velocimetry (PIV) and various sources of bathymetric information. *J. Hydrol*. **2017**, *554*, 490–506.
107. Dal Sasso SF, Pizarro A, Manfreda S. Metrics for the quantification of seeding characteristics to enhance image velocimetry performance in rivers. *Remote Sens.* **2020**, *12*, 1789.
108. Hauet A, Creutin JD, Belleudy P. Sensitivity study of large-scale particle image velocimetry measurement of river discharge using numerical simulation. *J. Hydrol.* **2008**, *349*, 178–190.
109. Lewis QW, Rhoads BL. Resolving two-dimensional flow structure in rivers using large-scale particle image velocimetry: An example from a stream confluence. *Water Resour. Res.* **2015**, *51*, 7977–7994.
110. Pumo D, Noto LV, Viola F. Ecohydrological modelling of flow duration curve in Mediterranean river basins. *Adv. Water Resour*. **2013**, *52*, 314–327.
111. Gena AW, Voelker C, Settles GS. Qualitative and quantitative schlieren optical measurement of the human thermal plume. *Indoor Air* **2020**, *30*, 757–766.
112. Thielicke W, Sonntag R. Particle Image Velocimetry for MATLAB: Accuracy and enhanced algorithms in PIVlab. *J. Open Res. Softw*. **2021**, *9*, 1–14.
113. Tauro F, Pagano C, Phamduy P, Grimaldi S, Porfiri M. Large-scale particle image velocimetry from an unmanned aerial vehicle. *IEEE ASME Trans. Mechatron.* **2015**, *20*, 3269–3275.
114. Saumier LP, Khouider B, Agueh M. Optimal transport for particle image velocimetry: real data and postprocessing algorithms. *SIAM J. Appl. Math.* **2015**, *75*, 2495–2514.
115. Sarno L, Carravetta A, Tai YC, Martino R, Papa MN, Kuo CY. Measuring the velocity fields of granular flows–Employment of a multi-pass two-dimensional particle image velocimetry (2D-PIV) approach. *Adv. Powder Technol.* **2018**, *29*, 3107–3123.
116. Pumo D, Alongi F, Ciraolo G, Noto LV. Optical Methods for River Monitoring: A Simulation-Based Approach to Explore Optimal Experimental Setup for LSPIV. *Water* **2021**, *13*, 247.
117. Garcia D. Robust smoothing of gridded data in one and higher dimensions with missing values. *Comput. Stat. Data Anal.* **2010**, *54*, 1167–1178.
118. Nogueira J, Lecuona A, Rodriguez PA. Data validation, false vectors correction and derived magnitudes calculation on PIV data. *Meas. Sci. Technol.* **1997**, *8*, 1493.
119. Yao M, Nan J, Chen T. Effect of particle size distribution on turbidity under various water quality levels during flocculation processes. *Desalination* **2014**, *354*, 116–124.
120. Kaldellis JK, Kondili EM. The water shortage problem in the Aegean archipelago islands: Cost-effective desalination prospects. *Desalination* **2007**, *216*, 123–138.
121. Stathi E, Kastridis A, Myronidis D. Analysis of Hydrometeorological Characteristics and Water Demand in Semi-Arid Mediterranean Catchments under Water Deficit Conditions. *Climate* **2023**, *11*, 137.
122. Stream Assessment and Mitigation Protocols: A Review of Commonalities and Differences. Available online: https://www.epa.gov/sites/default/files/2015-07/documents/stream_protocols_2010.pdf (accessed on 6 June 2022).
123. Gkiatas G, Kasapidis I, Koutalakis P, Iakovoglou V, Savvopoulou A, Germantzidis I, et al. Enhancing urban and sub-urban riparian areas through ecosystem services and ecotourism activities. *Water Supply* **2021**, *21*, 2974–2988.
124. Latsiou A, Kouvarda T, Stefanidis K, Papaioannou G, Gritzalis K, Dimitriou E. Pressures and status of the riparian vegetation in Greek rivers: Overview and preliminary assessment. *Hydrology* **2021**, *8*, 55.
125. Arnell NW, Gosling SN. The impacts of climate change on river flow regimes at the global scale. *J. Hydrol.* **2013**, *486*, 351–364.
126. Schneider C, Laizé CLR, Acreman MC, Flörke M. How will climate change modify river flow regimes in Europe? *Hydrol. Earth Syst. Sci.* **2013**, *17*, 325–339.
127. Fernández D, Barquin J, Raven P. A review of river habitat characterisation methods: indices vs. characterisation protocols. *Limnetica* **2011**, *30*, 0217–0234.
128. Belletti B, Rinaldi M, Buijse AD, Gurnell AM, Mosselman E. A review of assessment methods for river hydromorphology. *Environ. Earth Sci.* **2015**, *73*, 2079–2100.
129. MPCA Stream Habitat Assessment (MSHA) Protocol for Stream Monitoring Sites. Available online: https://www.pca.state.mn.us/sites/default/files/wq-bsm3-02.pdf (accessed on 6 June 2022).
130. Woodget AS, Austrums R, Maddock IP, Habit E. Drones and digital photogrammetry: from classifications to continuums for monitoring river habitat and hydromorphology. *Wiley Interdiscip. Rev. Water* **2017**, *4*, e1222.
131. Monteiro JG, Jiménez JL, Gizzi F, Přikryl P, Lefcheck JS, Santos RS, et al. Novel approach to enhance coastal habitat and biotope mapping with drone aerial imagery analysis. *Sci. Rep*. **2021**, *11*, 1–13.
132. Rivas Casado M, Ballesteros Gonzalez R, Wright R, Bellamy P. Quantifying the effect of aerial imagery resolution in automated hydromorphological river characterisation. *Remote Sens*. **2016**, *8*, 650.
133. Hooper L, Hubbart JA. A rapid physical habitat assessment of wadeable streams for mixed-land-use watersheds. *Hydrology* **2016**, *3*, 37.
134. Boitsidis AJ, Gurnell AM, Scott M, Petts GE, Armitage PD. A decision support system for identifying the habitat quality and rehabilitation potential of urban rivers. *Water Environ. J.* **2006**, *20*, 130–140.
135. Munné A, Prat N, Solà C, Bonada N, Rieradevall M. A simple field method for assessing the ecological quality of riparian habitat in rivers and streams: QBR index. *Aquat. Conserv. Mar. Freshw. Ecosyst.* **2003**, *13*, 147–163.

136. Richter BD, Baumgartner JV, Powell J, Braun DP. A method for assessing hydrologic alteration within ecosystems. *Conserv. Biol.* **1996**, *10*, 1163–1174.
137. Palau A, Alcázar J. The basic flow method for incorporating flow variability in environmental flows. *River Res. Appl.* **2012**, *28*, 93–102.
138. Clarke RT, Lorenz A, Sandin L, Schmidt-Kloiber A, Strackbein J, Kneebone NT, et al. Effects of sampling and sub-sampling variation using the STAR-AQEM sampling protocol on the precision of macroinvertebrate metrics. In *The Ecological Status of European Rivers: Evaluation and Intercalibration of Assessment Methods*; Springer: Dordrecht, The Netherlands, 2006.
139. Healey M, Raine A, Parsons L, Cook N. *River Condition Index in New South Wales: Method Development and Application*; NSW Office of Water: Sydney, Australia, 2012.
140. Stamataki MD, Koutalakis P, Papadopoulos D, Tzoraki O. Protocols for the environmental monitoring of the coastal and transitional river ecosystems. In Proceedings of the 4th International Congress on Applied Ichthyology & Aquatic Environment—HydroMedit (Virtual), Mytilene, Greece, 4–6 November 2021.
141. Rivas Casado M, González RB, Ortega JF, Leinster P, Wright R. Towards a transferable UAV-based framework for river hydromorphological characterization. *Sensors* **2017**, *17*, 2210.
142. Tabacchi E, Lambs L, Guilloy H, Planty-Tabacchi AM, Muller E, Decamps H. Impacts of riparian vegetation on hydrological processes. *Hydrol. Process.* **2000**, *14*, 2959–2976.
143. Dosskey MG, Vidon P, Gurwick NP, Allan CJ, Duval TP, Lowrance R. The role of riparian vegetation in protecting and improving chemical water quality in streams. *J. Am. Water Resour. Assoc.* **2010**, *46*, 261–277.
144. Rajib A, Kim IL, Golden HE, Lane CR, Kumar SV, Yu Z, et al. Watershed modeling with remotely sensed big data: MODIS leaf area index improves hydrology and water quality predictions. *Remote Sens*. **2020**, *12*, 2148.
145. Zaimes GN, Gounaridis D, Fotakis D. Assessing riparian land-uses/vegetation cover along the Nestos river in Greece. *Fresenius Environ. Bull.* **2011**, *20*, 3217–3225.
146. Simmons T, Armstrong T, Hawkins CP. Using aquatic invertebrates to measure the health of stream ecosystems: New bioassessment tools for Alaska's parklands. *Alaska Park Sci.* **2021**, *20*, 96–103.
147. Stefanidis K, Papastergiadou E. Linkages between macrophyte functional traits and water quality: insights from a study in freshwater lakes of Greece. *Water* **2019**, *11*, 1047.
148. Nihei Y, Kimizu A. A new monitoring system for river discharge with horizontal acoustic Doppler current profiler measurements and river flow simulation. *Water Resour. Res.* **2008**, *44*, doi:10.1029/2008WR006970.
149. Reichl F, Hack J. Derivation of flow duration curves to estimate hydropower generation potential in data-scarce regions. *Water* **2017**, *9*, 572.
150. Blasch KW, Ferré TP, Christensen AH, Hoffmann JP. New field method to determine streamflow timing using electrical resistance sensors. *Vadose Zone J.* **2002**, *1*, 289–299.
151. What is the difference between land cover and land use? Available online: https://oceanservice.noaa.gov/facts/lclu.html (accessed on 20 January 2023).
152. Poikane S, Herrero FS, Kelly MG, Borja A, Birk S, van de Bund W. European aquatic ecological assessment methods: A critical review of their sensitivity to key pressures. *Sci. Total Environ.* **2020**, *740*, 140075.